Autodisplay of α-amylase from *Bacillus megaterium* in *E. coli* for the bioconversion of starch to hydrogen, ethanol and succinic acid

Ana K. Gutiérrez-García[a1], Cecilia L. Alvarez-Guzmán[a1], Antonio De Leon-Rodriguez[a*]

[a]División de Biología Molecular, Instituto Potosino de Investigación Científica y Tecnológica, A.C., Camino a la Presa San José 2055, Col. Lomas 4ª Sección, C.P. 78216 San Luis Potosí, SLP, México.

Submitted to: Enzyme Microbial. Technol.

*Corresponding author:aleonr@me.com, aleonr@ipicyt.edu.mx

[1]These authors contributed equally.

Abstract

In this work, the expression of a α-amylase from *Bacillus megaterium* on the cell surface of *E. coli* strains WDHA (Δ*hyc*A, Δ*ldh*A) and WDHFP (Δ*hyc*A, Δ*frd*D and Δ*pta*) by the autodisplay AIDA system was carried out to confer the ability to the *E. coli* strains to produce hydrogen, ethanol and succinic acid from starch. For the characterization of the α-amylase, the effect of temperature (30-70°C), pH (3-6) and $CaCl_2$ concentration (0-25 mM) as well as the thermostability of the enzyme under different temperatures (55-80°C) at several time intervals (0-15 min) were evaluated. The results showed that the α-amylase has a maximum activity at 55°C and pH 4.5. Calcium is required for the activity as well for the thermal stability of the enzyme. The Km and Vmax values calculated were 5.8 mg/mL and 0.0106 mg/ml/min respectively. Furthermore, a set of batch fermentations were carried out using 10 g/L plus 1 g/L of glucose as carbon source in 120 mL anaerobically serological bottles using WDHA (succinate producer) or WDHFP (ethanol producer) *E. coli* strains harboring the pAIDA-amyA plasmid. The hydrogen and succinic acid production for WDHA was 1,056.06 mL/L and 6.8 g/L, respectively whereas WDHFP strain produced 1,689.68 mL/L of hydrogen and 2.8 g/L of ethanol. This work represents a promising strategy to improve the exploitation of starchy biomass for the production of valuable compounds without the need of a pre-saccharification process.

Keywords: Whole-cell catalysis; α-amylase; starch hydrolysis; biofuels

1. Introduction

The utilization of biomass as feedstock for the production of biofuels and bio-based chemicals has recently become an attractive alternative option. One of the main feedstocks for biofuel and chemicals production is the starch-rich biomass, which is easily depolymerized by amylases to generate high yields of glucose [1]. Starch is contained in many staple foods (e.g. potatoes, wheat, corn, rice, among others), therefore it is abundant and consists of a large number of glucose units conjugated with glycosidic bonds [2]. However, although starchy materials are available in abundance, a previous liquefaction and saccharification process of the biomass is required to hydrolyze polysaccharides into monosaccharides before its use for biofuel or chemical production. Amylases are extracellular enzymes, which hydrolyze starch molecules to give such diverse products as dextrins, and progressively smaller polymers composed of glucose units. In this regard, α-amylases are endoamylases catalyzing the hydrolysis of internal α-1,4-glycosidic linkages in starch in a random manner, preferably in immobilized form [3]. They are usually/mainly produced by bacteria belonging to the genus *Bacillus* such as *B. subtilis, B. licheniformis*, *B. amyloliquefancies* and *B. stearothemophilus* [4]. Several strategies have been adopted for the construction of starch-utilizing system, such as the addition of large amounts of amylases. The use of pure enzymes in biocatalysis has several advantages such as the specificity for selected reactions, simple equipment and procedures [5]. Nevertheless, enzyme production, isolation and purification can be expensive and in addition, the enzymes are often used only once which increases the cost of the process. On the contrary, the use of microorganisms as whole-cell biocatalysts avoids the purification steps and

allows the recycling of the enzymes. The advantages of the application of this technology is that the cells themselves provide a natural environment for the enzymes preventing conformational changes in the protein which could result in the loss of the activity [6]. Also, other important advantage is that they can efficiently regenerate the enzymes. Among the different whole-cell systems the AIDA (adhesin involved in diffuse adherence) autodisplay system from *Escherichia coli* have favorable features such as modularity and simplicity. This is an efficient surface display system for Gram-negative bacteria and is based on the autotransporter secretion pathway. In general, it consists of a cassette that includes the β barrel of AIDA, the recombinant passenger protein is transported simply introducing its coding sequence in the frame between the signal peptide and the translocator domain [7]. This autodisplay system offers the expression of more than 10^5 recombinant molecules per single cell, permits the multimerization of subunits expressed from monomeric genes at the cell surface and it results in a superior surface exposure of heterologous passenger [8].

The aim of this study is to carry out the fermentation of starch for the production of hydrogen, succinate or ethanol by two *E. coli* strains with deletions of genes related to carbon metabolism. To make this possible, we used the autodisplay AIDA system to express the α-amylase from *B. megaterium* in the cell surface of *E. coli*. The characterization of the enzyme activity, as well as the effectiveness of its ability to hydrolyze starch in batch fermentations was assessed.

2. Material and methods

2.1. Bacterial strain and growth conditions

Strains of *E. coli* WDH were mutated as previously described by Balderas-Hernandez, Maldonado [9]. Briefly, *E. coli* WDH strain [10] (Δ*hycA*, negative regulator of the formate regulon) was used as parental strain. Gene deletion was carried out by transduction with bacteriophage P1 [11]. Strains from single-gene knockout mutant collection of the nonessential genes of the *E. coli* W3110 were used as donors. Deleted genes were ***ldhA***: D-lactate dehydrogenase; ***frdD***: fumarate reductase; and ***pta***: phosphate acetyltransferase. Gene deletions and resistance loss were confirmed by PCR analysis using standard conditions and the primers described in Table 1.

E. coli Top 10 and pGEM-T easy vector which were used for subcloning of PCR products were obtained from Promega. Cells were routinely grown at 31°C in Luria-Bertani (LB) medium, containing 150 µg/mL of ampicillin. Solid media were prepared by the addition of agar (1.5% w/v).

2.2. Construction of artificial AIDA system

The design of the amyA-AIDA fusion gene was carried out to confer the ability of *E. coli* to degrade starch. For this, the DNA sequences were assembled with the Snapgene software (GSL Biotech LLC, Version 3.3) and MacVector (MacVector, Inc, Version 10.1). The design of the fusion genes for the *"autodisplay"* of proteins

was based on the AIDA sequence reported by Maurer [7]. For the translocation to the internal membrane, the signal peptide of the toxin of the β-subunit of *Vibrio cholerae* (CtxB) was selected. The autotransporter gene for AIDA was used, which consists of a peptide and a β-barrel (amino acids from 839 to 1286, GenBank: X65022.1). The nucleotide sequences were optimized for them expression in *E. coli* (GenScript, New Jerser, USA). The codon-optimization was performed by evading as many restriction sites as possible; strategic restriction sites were added to be able to exchange protein passenger when required. The gapAP1 promoter of the constitutive *gapA* gene of *E. coli* was selected as the transcriptional regulator of the amyA-AIDA gene, since it works under aerobic and anaerobic conditions. The construction was synthesized by the Biomatik Corp (Delaware, USA). The pUC57 plasmid was used as host and the *EcoR*V was used as restriction site as a cloning site. The artificial cassette was called pUC57-AIDA.

The *amyA* gene encoding for α-amylase was amplified by polymerase chain reaction of the *B. megaterium* genome (X07261.1). PCR product was inserted into pGEM-T easy vector and then it was digested using the restriction enzymes *Asc*I and *Xho*I before ligation into pUC57-AIDA plasmid, which was digested with the same enzymes. This yielded an in-frame fusion protein consisting of the CtxB signal peptide, α-amylase as the passenger, the linker region and the β-barrel autotransporter under the control of the gapAP1 promoter. The plasmid was transformed into *E. coli* WDHA and WDHFP by electroporation. The α-amylase gene has a length of 1500 bp. The inserted gene was sequenced before its use in the subsequent experiments.

2.3. α-Amylase activity visualization

The amylase activity was visually detected from the cleaning zone around the colonies on starch plates containing 0.3% meat extract, 0.2% soluble starch, 0.5% peptone and 1.5% of agar. The starch agar plate was seeded with individual colonies of *E. coli* WDHA/pAIDA-amyA as well as a negative control *E. coli* WDHA and incubated for 48 h at 37°C. Subsequently, the plate was flooded with iodine reagent (0.01 M I_2-KI solution) and washed with 1 M NaCl.

2.4. Enzymatic reaction

100 mL of LB medium with 200 µg/mL of ampicillin were inoculated with *E. coli* WDHA or WDHFP. Cells were cultured at 31°C and 180 rpm until an optical density at 600 nm ($O.D._{600nm}$) of 1 was reached. The cells were centrifuged and washed twice with reaction buffer. The enzymatic reaction was carried out in triplicate, with a biomass $O.D._{600nm}$ of 10 and using 1% soluble starch as substrate. The reactions were stopped by centrifugation at 13,000 rpm for 5 min and the supernatant was used to measure the enzymatic activity.

2.5. Temperature and pH effect on enzyme activity

The effect of temperature on the enzyme activity was determined by incubating the cells in acetate buffer pH 5.5 containing 1% starch and 5 mM $CaCl_2$ at temperatures ranging from 30 to 70°C for 30 min with vigorous shaking. The enzyme activity was then measured using the 3,5-dinitrosalicylic acid DNS method [12]. Effect of pH on the amylase activity was determined at different pH (3.5-6) using the universal Britton and Robinson´s buffer (50 mM phosphoric acid, 50 mM

158 boric acid and 50 mM acetic acid), 1% starch and 5 mM $CaCl_2$ at 55°C for 30 min.
159 A control without cells was used as a negative control.

160 **2.6. Determination of enzyme thermostability**

161 The thermal stability of the α-amylase activity was determined by measuring the
162 final activities of the enzyme after 15 to 60 min of incubation in acetate buffer pH
163 4.5 and temperature ranging from 55 to 80°C with and without 5 mM $CaCl_2$.

164 **2.7. Effect of calcium on enzyme activity**

165 To evaluate if the calcium influences the α-amylase activity, cells were incubated in
166 Britton and Robinson´s buffer pH 4.5 at 55°C for 30 min with calcium chloride
167 concentration ranging from 0 to 25 mM and vigorous shaking. The negative
168 controls were also evaluated. The activity assayed in the absence of calcium was
169 recorded as 100%.

170 **2.8. Determination of total reducing sugars**

171 The α-amylase activity was determined by measuring the reducing sugars released
172 during starch hydrolysis by DNS method [12]. The reaction mixture contained 50 µl
173 of supernatant from centrifuged samples and 150 µl of DNS reagent, the reaction
174 mixture was boiled for 5 min at 100°C and stopped by cooling to room temperature.
175 The absorbance was measured at 595 nm. Glucose served as the calibration
176 standard for total reducing sugar determination. 1 U was defined as the amount of
177 enzyme that releases 1 µmol of reducing sugars per minute and for the amylase
178 specific activity as one unit of amylase activity per mg of *E. coli* cells.

179 **2.9. Kinetic parameters calculation**

The maximum velocity (Vmax) and the Michaelis constant (Km) were calculated using the standard activity assay with different substrate concentration (0-3% w/v soluble starch) in Britton and Robinson´s buffer (pH 4.5) at 55°C. Kinetic constants (Km and Vmax) were calculated by the method of Lineweaver-Burk using standard linear regression techniques.

2.10. Hydrogen, succinate and ethanol production by the *E. coli* using soluble starch as substrate.

To conduct the hydrogen production by the *E. coli* WDH strains carrying the pAIDA-amyA plasmid using starch as carbon source, pre-inoculum was grown in LB medium (10 g/L peptone, 5 g/L Yeast extract, 5 g/L sodium chloride) supplemented with 200 µg/mL of ampicillin under aerobic conditions at 31°C for 16 h. Cells were harvested, centrifuged at 6000 rpm 10 min, washed and inoculated into 120 mL anaerobic serological bottles containing 110 mL of medium B (12.5 mg/L $Na_2MoO_4 \cdot 2H_2O$, 15 mg/L $MnSO_4 \cdot 7H_2O$, $CoCl_2 \cdot 8H_2O$ 3 mg/L, 75 mg/L $ZnCl_2$, 4500 mg/L $NH_4H_2PO_4$, 11,867 mg/L Na_2HPO_4, 125 mg/L K_2HPO_4, 100 mg/L $MgCl_2 \cdot 6H_2O$, 25 mg/L $FeSO_4 \cdot 6H_2O$, 5 mg/L $CuSO_4 \cdot 5H_2O$) [13], 0.5 g/L $CaCl_2$, 1 mL/L trace elements solution (ref), 1 g/L yeast extract (Difco), 1 g/L glucose and 10 g/L soluble starch. The cultures were started at pH 7.5 and were incubated at 31°C and 180 rpm. The experiments were carried out in triplicate.

2.11. Analytical methods

The amount of hydrogen produced was measured by the acidic water displacement method in an inverted burette connected to serological bottles with

rubber and a needle. The hydrogen percentage on the biogas was determined by gas chromatography using a thermal conductivity detector (Agilent Technologies Wilmington, DE, USA) as described elsewhere [10]. Samples of 1 mL were taken at different times during fermentation, and then cells were separated by 5 min centrifugation at 13000 rpm. The supernatants were filtered through a 0.22 µm membrane (Millipore, Bedford, Massachusetts, USA) [14]. Concentrations of soluble metabolites such as succinic acid, lactic acid, acetic acid, formic acid and ethanol were analyzed by High Performance Liquid Chromatography (HPLC, Infinity LC 1220, Agilent Technologies, Santa Clara CA, USA) using a Refraction Index Detector, a column Phenomenex Rezex ROA (Phenomenex Torrance, CA, USA) at 60°C, and 0.0025 M H_2SO_4 as mobile phase at 0.5 mL/min. An $O.D._{600nm}$ of 1.0 was equivalent to 0.37 g (dry cell weight, DCW) cells/L. Total sugar concentrations were measured using the phenol-sulfuric acid method [15].

3. Results and discussion

3.1. Design of AIDA system

The fusion gene (Fig. 1) consists of 5 'to 3' as follows: *Sma*I restriction site, 5' homologous recombination arm with target to the *frdABCD* gene, *EcoR*I restriction site, promoter of the *gapA* gene of *E .coli*, *Nde*I restriction site, CtxB protein signal peptide, *Asc*I restriction site, passenger gene *amyA* that encodes the α-amylase from *B. megaterium*, *Xho*I restriction site, linker and β-barrel of the AIDA autotransporter of *E. coli*, *Bam*HI restriction site, Rho Independent Terminator and *Sma*I restriction site. The cassette was inserted into the pUC57 plasmid at the

224 *Eco*RV restriction site. The resulting plasmid was called pAIDA-amyA and has a
225 size of 5934 bp.

226 **3.2. Detection of amylolytic activity on plate**

227 An initial plate assay was performed to determine whether the transformants
228 gained amylolytic activity. The amylolytic activity was observed by a halo formation
229 on agar plate. Cells carrying the plasmid pAIDA-amyA or the strain without it as a
230 control were inoculated on a plate of medium containing soluble starch. After
231 incubation for two days at 37°C, the plate was stained with iodine solution. The
232 result shown in figure 2, demonstrated that the cells harboring the plasmid pAIDA-
233 amyA hydrolyzed starch and produced a halo strictly around the colony, while no
234 halo formation was observed around the control cells. This assay indicated that the
235 former cells presented amylolytic activity due to the expression of the α-amylase
236 AIDA system.

237 **3.3. Effect of temperature and pH on enzyme activity**

238 The effect of temperature on the immobilized α-amylase activity was determined by
239 assaying enzyme activity at different temperatures in a range of 30 to 70°C (Fig.
240 3A). The gradual increase in temperature from 30 to 50°C increased the activity of
241 the α-amylase until 55 °C where the maximum activity was achieved. The activity
242 at 50 and 60°C showed over 70% of the maximum activity, however, a further
243 increase in temperature caused a detrimental effect on the activity, in spite of that,
244 the anchored-α-amylase remain active until 70°C. The optimum temperature of
245 amylase in this study was similar to other bacterial α-amylase such as *B.*
246 *stearothermophilus* or *Lactobacillus manihotivorans* LMG 18010 [16]. On the other

hand, the influence of pH on the α-amylase activity was evaluated at various pH values in a range of 3 to 6.5. As shown in figure 3B, the enzyme had the maximum activity at 4.5 and α-amylase activity declined rapidly at pH below 5.0 showing only about 30% activity was retained at pH 6. The maximum α-amylase activity at temperature (55°C) and optimum pH (4.5) was 60.17 U with the maximum specific α-amylase activity of 162.63 U/g. The optimum pH of α-amylases produced by several bacterial sources has been reported, including *Bacillus sp*, and they show a variety of pH profiles [17]. Being, the optimal pH of α-amylases in a range from 2 to 12 [17]. The maximum activity of most of these α-amylases is in the range of pH 6.0-8.0 [18-20] or pH 5.0-7.0 [21], but also has been reported α-amylases with maximum activity at low pH such as those produced by *Bacillus sp.* KR-8104 [22]. Acidic, neutral and alkaline α-amylases are suited to different industrial applications. Since optimum activity is obtained at low pH values, this enzyme is highly attractive for industrial process, because several industries applications take place at low pH values. Majority of the α-amylases are unstable at low pH and the liquefaction step in the starch process is currently constrained to operate at pH 5.8-6.2 and natural pH of starch slurry is generally around 4.5 (which is the optimum pH of the enzyme in this study). The extreme conditions required for such pretreatment necessitate the use of an enzyme that is resistant to low pH [23]. Since both, the prior and post process steps take place at pH 4.5, therefore, if the α-amylase is stable and active at low pH values one can omit the pH adjustment steps, which is very important in the processing [22].

3.4. Thermostability of the α-amylases

To determine the thermostability of the immobilized enzyme, cells were preincubated at different temperatures (55 to 80°C) with and without 5 mM $CaCl_2$ at different time intervals (15 to 60 min). The reaction mixture without calcium decreased in general around 60% of the maximum relative activity (Fig. 4). When the enzyme was preincubated at 55°C for 60 min of incubation, the activity decreased only 20% in the presence of calcium, interestingly the enzyme without calcium after 60 min of incubation decreased 60% of the maximum activity. At 60°C with calcium we observed a decreased of almost 60% after 60 min of incubation. On the other hand, at 60°C without calcium we observed a decreased of almost 60% of the activity after 15 min of incubation. In addition, the α-amylase activity was almost inactivated at 80°C after 60 min of incubation showing a remaining activity of 20%. All these findings indicated that Ca^{2+} ions are important for the folding and stability of the enzyme. It is known that the Ca^{2+} ion strongly influences the α-amylase activity, the positive effect of this metal ion on the thermostability of enzymes has been shown by several authors including on the α-amylases from *B. licheniformis* and *Pyrococcus furiosus* [24, 25]. Most of the α-amylases are reported to have one or two intrinsic Ca^{2+} ions. Secondary calcium binding site have also been reported, which enhanced the thermostability [23]. For instance, Saboury [26], reported the presence of different secondary binding sites for calcium in α-amylase of *B. amyloliquefaciens*, which were responsible for stabilization of the enzyme against thermal denaturation. The stabilizing effect of Ca^{2+} on thermostability can be explained due to the salting out of hydrophobic residues by Ca^{2+} in the protein, thus, causing the adoption of a compact structure [27].

3.5. Effect of calcium on α-amylase activity

The effect of calcium concentration was also evaluated (Fig. 5), the presence of 5 mM of $CaCl_2$ significatively increased the activity almost 50% compared to the control without calcium (p<0.05) and interestingly at 25 mM of $CaCl_2$ compared to the concentration of 5 mM the relative activity of α-amylase significatively increased 20% (p<0.05). This increase can be explained due to the fact that most of the α-amylases are metal ion-dependent enzymes, such as Ca^{2+}, and it has been reported that the addition of Ca^{2+} ions increases the α-amylase activity, as the alkaliphilic *Bacillus sp.* ANT-6 [23, 24].

3.6. Kinetic parameters of α-amylase

The kinetic parameters (Km and Vmax) of α-amylase with soluble starch as substrate were determined by the inverse reciprocal of Lineweaver-Burk. The Km and Vmax values were 5.8 mg/mL and 0.0106 mg/mL/min respectively (Fig. 6). So far there are no reports of catalytic constants of α-amylases for whole-cell biocatalysis, but there are reports of α-amylases anchored to nanoparticles or free α-amylases. The Km value for starch of the α-amylase of this study was within the range of many amylases reported (Table 2) [16].

3.7. Production of hydrogen, succinate and ethanol from soluble starch

To evaluate the effectiveness of the α-amylase-AIDA display system on the production of hydrogen succinate and ethanol by the *E. coli* strain WDHA/pAIDA-amyA, a set of batch cultures was carried out. Cells at an initial biomass concentration of 0.037 g/L were cultivated anaerobically with 10 g/L soluble starch

316 and 1 g/L of glucose as carbon source. The results shown that cells carrying the
317 plasmid pAIDA-amyA, were able to utilize the starch in the medium as carbon
318 source. As it can be seen in figure 7A, *E. coli* WDHA/pAIDA-amyA proliferated to
319 reach a maximum biomass of 0.92 g/L at the 24 h with an adaptation phase of 12
320 h. During this lag phase, it is assumed that the WDHA/pAIDA-amyA strain used the
321 small amount of glucose (1 g/L) available in the medium to support the cellular
322 growth and hence the α-amylase synthesis. After this phase, the cell surface-
323 anchored α-amylases reacted hydrolyzing the starch available releasing the
324 reducing sugars needed for the cellular growth. Also, with the concomitant cellular
325 growth, hydrogen and several soluble metabolites were produced. Figure 7A
326 reveals that hydrogen production began at the 12 h and increased as the total
327 sugar concentration decreased to reach a maximum hydrogen production of
328 1,056.06 mL/L after 82 h of fermentation and a hydrogen production rate of 26.8
329 mL/L/h. *E. coli* WDHA strain has deleted the *hyc*A gene which encodes for the
330 negative regulator for the formate regulon [10], as well as the deletion of *ldh*A gene
331 which encodes for a NAD-linked lactate dehydrogenase enzyme responsible for
332 the lactic acid production [28]. In this work, the analysis of the metabolic products
333 formed during the fermentation (Fig. 8) shows that the less abundant product was
334 lactic acid (0.7 g/L) while formic acid was not detected in the medium. On the other
335 hand, succinic acid was the main soluble metabolite (6.8 g/L), followed by the
336 production of acetic acid (1.7 g/L) and ethanol (1.3 g/L). Since, succinic acid
337 production competes with the hydrogen and ethanol production, a WDH $frdD^-$ pta^-
338 mutant was generated and transformed with the pAIDA-amyA plasmid
339 (WDHFP/pAIDA-amyA) to improve the flux of pyruvate to the hydrogen and ethanol

production without acetic acid formation. *frd*D gene encodes for the fumarate reductase [29], whereas *pta* gene encodes for the phosphate acetyltransferase which is the first enzyme of the acetate pathway [30]. In figure 7B, it is noted that the hydrogen production and cellular growth by WDHFP/pAIDA-amyA strain presented a longer lag phase compared to the WDHA/pAIDA-amyA strain, this behavior can be attributed to the *pta* gene deletion. Chang et al. [30] reported the same effect in their study, where a *E. coli* JP231 strain which has deleted the *pta* gene showed a slower growth rate on various carbon sources compared to those of the wild type strain, the authors attributed this conduct to the perturbation of the pyruvate and acetyl CoA fluxes in the mutant. It has been previously described that when *pta* is deleted in *E. coli*, pyruvate accumulates in the cell, consequently, the pyruvate accumulation will lower the Phosphoenol pyruvate (PEP)/pyruvate ratio, which results in a lowered substrate consumption of the sugars transported by the phosphotransferase system (PTS) which requires PEP [30-32]. After 35 h, WDHFP/pAIDA-amyA started the hydrogen production and continued until the 116 h of fermentation, where the maximum hydrogen production of 1,689.68 mL/L was achieved with a production rate of 33.14 mL/L/h. This hydrogen production is 60% higher than the one attained by WDHA, as well as the production rate. In figure 7B it is observed that the total sugar concentration decreases with the simultaneous hydrogen production increment, hence this data confirms the effectiveness hydrolysis of starch in the medium and its use as carbon source. Regarding to the metabolites produced in the fermentation, in figure 8 it can be observed that the metabolite distribution changed with respect to the profile showed by WDHA/pAIDA-amyA. In this case, the succinic acid reached a concentration of 2.3

g/L, whereas acetic acid 2.2 g/L, since *frd*D and *pta* genes were deleted from WDHFP/pAIDA-amyA we expected to observe no succinic and acetic acid production, however, there are alternative routes for the production of these acids in *E. coli*, which involves the glyoxylate shunt where succinic acid is formed from acetyl Co-A by the isocitrate lyase (aceA), and acetic acid can be produced directly from pyruvate by the pyruvate oxidase (poxB) [33]. Furthermore, the ethanol production reached a concentration of 2.8 g/L which is approximately twice the production achieved by WDHA/pAIDA-amyA. The results showed that the cell-surface α-amylase synthesis by the AIDA system is an effective alternative for the use of a complex polysaccharide such as starch by *E. coli* without the requirement of a saccharification pre-treatment. Moreover, the ability of *E. coli* WDHA and WDHFP carrying the pAIDA-amyA plasmid for the of biofuels production like hydrogen and ethanol, as well as succinic acid which is an important building block in chemical industry shows the potential for these strains to be applied in industrial processes using starch-rich biomass.

4. Conclusions

In this work, we combined a cell surface display system and metabolic engineering for the overproduction of hydrogen, succinate and ethanol using a cheap and abundant polysaccharide such as starch. The expression of α-amylase enzymes on the cell surface of metabolic engineered *E. coli* strains using the AIDA autodisplay system is a novel tool for the hydrolysis of starch and agroindustrial wastes, with this system it is possible to reduce the costs of the production of enzymes and the efficiency of the process.

5. Acknowledgments

Cecilia Alvarez and A. Gutiérrez, thanks the National Council of Science and Technology (CONACYT) for their scholarships 330870, 297341, respectively. We thank Victor E. Balderas for his technical support.

Funding: This work was supported by CONACyT Ciencias básicas 281700.

6. References

1. Tanaka, T. and A. Kondo, *Cell surface engineering of industrial microorganisms for biorefining applications.* Biotechnology advances, 2015. **33**(7): p. 1403-1411.
2. Yamamoto, K., et al., *Starchy biomass-powered enzymatic biofuel cell based on amylases and glucose oxidase multi-immobilized bioanode.* New biotechnology, 2013. **30**(5): p. 531-535.
3. Gupta, R., et al., *Microbial α-amylases: a biotechnological perspective.* Process biochemistry, 2003. **38**(11): p. 1599-1616.
4. Nigam, P. and D. Singh, *Enzyme and microbial systems involved in starch processing.* Enzyme and Microbial Technology, 1995. **17**(9): p. 770-778.
5. De Carvalho, C.C., *Enzymatic and whole cell catalysis: finding new strategies for old processes.* Biotechnology advances, 2011. **29**(1): p. 75-83.
6. Schüürmann, J., et al., *Bacterial whole-cell biocatalysts by surface display of enzymes: toward industrial application.* Applied microbiology and biotechnology, 2014. **98**(19): p. 8031-8046.
7. Maurer, J., J. Jose, and T.F. Meyer, *Characterization of the essential transport function of the AIDA-I autotransporter and evidence supporting structural predictions.* Journal of bacteriology, 1999. **181**(22): p. 7014-7020.
8. Bielen, A., et al., *Microbial anchoring systems for cell-surface display of lipolytic enzymes.* Food Technology and Biotechnology, 2014. **52**(1): p. 16-34.
9. Balderas-Hernandez, V.E., et al., *Improvement of hydrogen production by metabolic engineering of Escherichia coli: Modification on both the PTS system and central carbon metabolism.* International Journal of Hydrogen Energy, 2019.
10. Rosales-Colunga, L.M., et al., *Hydrogen production by Escherichia coli ΔhycA ΔlacI using cheese whey as substrate.* international journal of hydrogen energy, 2010. **35**(2): p. 491-499.
11. Thomason, L.C., N. Costantino, and D.L. Court, *E. coli genome manipulation by P1 transduction.* Current protocols in molecular biology, 2007. **79**(1): p. 1.17. 1-1.17. 8.
12. Miller, G.L., *Use of dinitrosalicylic acid reagent for determination of reducing sugar.* Analytical chemistry, 1959. **31**(3): p. 426-428.
13. Davila-Vazquez, G., et al., *The buffer composition impacts the hydrogen production and the microbial community composition in non-axenic cultures.* Biomass and bioenergy, 2011. **35**(7): p. 3174-3181.

14. Lopez-Hidalgo, A.M., A. Sánchez, and A. De León-Rodríguez, *Simultaneous production of bioethanol and biohydrogen by Escherichia coli WDHL using wheat straw hydrolysate as substrate.* Fuel, 2017. **188**: p. 19-27.
15. Masuko, T., et al., *Carbohydrate analysis by a phenol–sulfuric acid method in microplate format.* Analytical biochemistry, 2005. **339**(1): p. 69-72.
16. Aguilar, G., et al., *Purification and characterization of an extracellular α-amylase produced by Lactobacillus manihotivorans LMG 18010T, an amylolytic lactic acid bacterium.* Enzyme and Microbial Technology, 2000. **27**(6): p. 406-413.
17. Sharma, A. and T. Satyanarayana, *Microbial acid-stable α-amylases: characteristics, genetic engineering and applications.* Process Biochemistry, 2013. **48**(2): p. 201-211.
18. Najafi, M.F., D. Deobagkar, and D. Deobagkar, *Purification and characterization of an extracellular α-amylase from Bacillus subtilis AX20.* Protein expression and purification, 2005. **41**(2): p. 349-354.
19. Robyt, J.F. and R.J. Ackerman, *Isolation, purification, and characterization of a maltotetraose-producing amylase from Pseudomonas stutzeri.* Archives of biochemistry and biophysics, 1971. **145**(1): p. 105-114.
20. Malhotra, R., S. Noorwez, and T. Satyanarayana, *Production and partial characterization of thermostable and calcium-independent α-amylase of an extreme thermophile Bacillus thermooleovorans NP54.* Letters in Applied Microbiology, 2000. **31**(5): p. 378-384.
21. Pandey, A., et al., *Advances in microbial amylases.* Biotechnology and applied biochemistry, 2000. **31**: p. 135-152.
22. Sajedi, R.H., et al., *A Ca-independent α-amylase that is active and stable at low pH from the Bacillus sp. KR-8104.* Enzyme and Microbial Technology, 2005. **36**(5-6): p. 666-671.
23. Sivaramakrishnan, S., et al., *α-Amylases from microbial sources–an overview on recent developments.* Food Technol Biotechnol, 2006. **44**(2): p. 173-184.
24. Burhan, A., et al., *Enzymatic properties of a novel thermostable, thermophilic, alkaline and chelator resistant amylase from an alkaliphilic Bacillus sp. isolate ANT-6.* Process Biochemistry, 2003. **38**(10): p. 1397-1403.
25. Brown, S.H. and R.M. Kelly, *Characterization of amylolytic enzymes, having both α-1, 4 and α-1, 6 hydrolytic activity, from the thermophilic archaea Pyrococcus furiosus and Thermococcus litoralis.* Appl. Environ. Microbiol., 1993. **59**(8): p. 2614-2621.
26. Saboury, A.A., *Stability, activity and binding properties study of α-amylase upon interaction with Ca2+ and Co2+.* Biologia, 2002. **57**(11): p. 221-228.
27. Goyal, N., J. Gupta, and S. Soni, *A novel raw starch digesting thermostable α-amylase from Bacillus sp. I-3 and its use in the direct hydrolysis of raw potato starch.* Enzyme and Microbial Technology, 2005. **37**(7): p. 723-734.
28. Bunch, P.K., et al., *The IdhA gene encoding the fermentative lactate dehydrogenase of Escherichia coli.* Microbiology, 1997. **143**(1): p. 187-195.
29. Westenberg, D.J., et al., *Escherichia coli fumarate reductase frdC and frdD mutants. Identification of amino acid residues involved in catalytic activity with quinones.* Journal of Biological Chemistry, 1993. **268**(2): p. 815-822.
30. Chang, D.-E., et al., *Acetate metabolism in a pta mutant ofescherichia coli w3110: Importance of maintaining acetyl coenzyme a flux for growth and survival.* Journal of bacteriology, 1999. **181**(21): p. 6656-6663.
31. Castaño-Cerezo, S., et al., *An insight into the role of phosphotransacetylase (pta) and the acetate/acetyl-CoA node in Escherichia coli.* Microbial cell factories, 2009. **8**(1): p. 54.

32. Zhu, J. and K. Shimizu, *Effect of a single-gene knockout on the metabolic regulation in Escherichia coli for D-lactate production under microaerobic condition.* Metabolic engineering, 2005. **7**(2): p. 104-115.
33. Wu, H., et al., *Improved succinic acid production in the anaerobic culture of an Escherichia coli pflB ldhA double mutant as a result of enhanced anaplerotic activities in the preceding aerobic culture.* Appl. Environ. Microbiol., 2007. **73**(24): p. 7837-7843.
34. Salgaonkar, M., S.S. Nadar, and V.K. Rathod, *Combi-metal organic framework (Combi-MOF) of α-amylase and glucoamylase for one pot starch hydrolysis.* International journal of biological macromolecules, 2018. **113**: p. 464-475.
35. Klapiszewski, Ł., J. Zdarta, and T. Jesionowski, *Titania/lignin hybrid materials as a novel support for α-amylase immobilization: A comprehensive study.* Colloids and Surfaces B: Biointerfaces, 2018. **162**: p. 90-97.
36. Dey, G., et al., *Purification and characterization of maltooligosaccharide-forming amylase from Bacillus circulans GRS 313.* Journal of Industrial Microbiology and Biotechnology, 2002. **28**(4): p. 193-200.

Table 1. *E. coli* strains and primers used in this study

Strains Name	Genotype description	Reference
WDH	Escherichia coli (lac^+, gal^+, F^-, λ^-, IN (rrnD-rrnE)1, rph-1) Δ*hycA*	[10]
WDHA	WDH Δ*ldhA*	This work
WDHFP	WDH Δ*frdD* Δ*pta*	This work
Primers Name	**Sequence (5´to 3´)**	**Reference**
ldhA-FCK	TCGCCATCGGTCTACGGGC	[9]
ldhA-RCK	CATAACACCATTAGCGAAAT	
frdD-FCK	TCTGGTTTCCATACAA	
frdD-RCK	TTAGATTGTAACGACACCAATC	
pta-FCK	CTGCACGTTTCGGCAAATCT	This work
pta-RCK	ATTGCGGACATAGCGCAAAT	This work

491 **Table 2. Kinetic parameters of α-amylases by diverse types of**
492 **immobilizations**

Biocatalysis	Autotransporter	Vmax	Km	Reference
Immobilization	Combi-MOF	6.9881±0.14 µmol/min	0.5889±0.053 µM	[34]
Immobilization	Biopolymer	855 U/mg	15.03 mM	[35]
Bacillus circulans GRS 313	Free enzyme	68.97 U/min	11.66 mg/mL	[36]
Whole cell catalysis	AIDA	0.0106 mg/mL/min	5.8 mg/mL	This work

493

Figure captions

Figure 1. Structure of autodisplay AIDA system. It consists of a signal peptide (derived from CtxB), followed by the gene encode for α-amylase. Subsequently, the linker and the β-barrel.

Figure 2. A starch agar plate showing α-amylase activity by (A) *E. coli* WDHA/pAIDA-amyA strain. (B) Negative control *E. coli* WDHA. The strains were cultured on a starch agar plate for 48 h at 37°C.

Figure 3. Effect of temperature and pH on α-amylase activity. (A) Temperature dependence of α-amylase. (B) Relative activity profile of α-amylase at different pH conditions. Values are expressed as mean of percentage of relative activity. Bars represent means ± standard deviations for three replicates.

Figure 4. Thermal stability of α-amylase. For the determination of the thermostability of α-amylase, the enzyme was pre-incubated at different temperatures for 15 to 60 min in the presence or absence of 5 mM $CaCl_2$ and the remaining activity was determined incubating the enzyme at optimum temperature (55°C for 30 min). Bars represent means ± standard deviations for three replicates.

Figure 5. Effect of $CaCl_2$ concentration on α-amylase activity. Continue line represent reaction mixture with 5 mM $CaCl_{2;}$ dotted line represents the reaction mixture without $CaCl_2$ n=3 (p<0.05)

Figure 6. Michaelis-Menten type plot of α-amylase hydrolysis rate at different starch concentration**.**

Figure 7. Kinetics of hydrogen production, cell growth and total sugar consumption by (A) WDHA/pAIDA-amyA and (B) WDHFP/pAIDA-amyA using 10 g/L of starch and 1 g/L of glucose incubated at 31°C, initial pH 7.5 and 180 rpm.

Figure 8. Fermentative metabolites produced at the end of each fermentation.

519

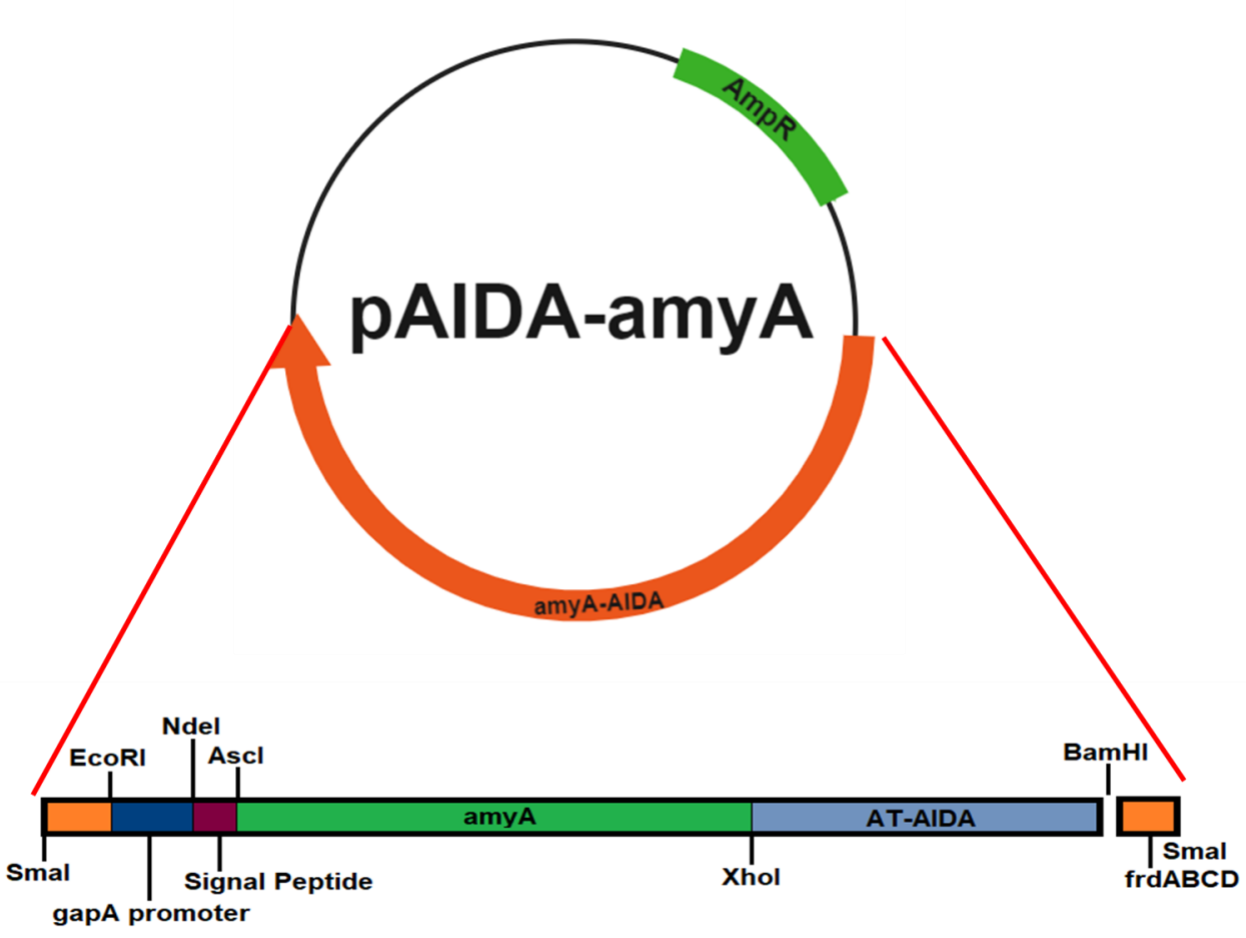

520

521 **Fig. 1**

522

523

524

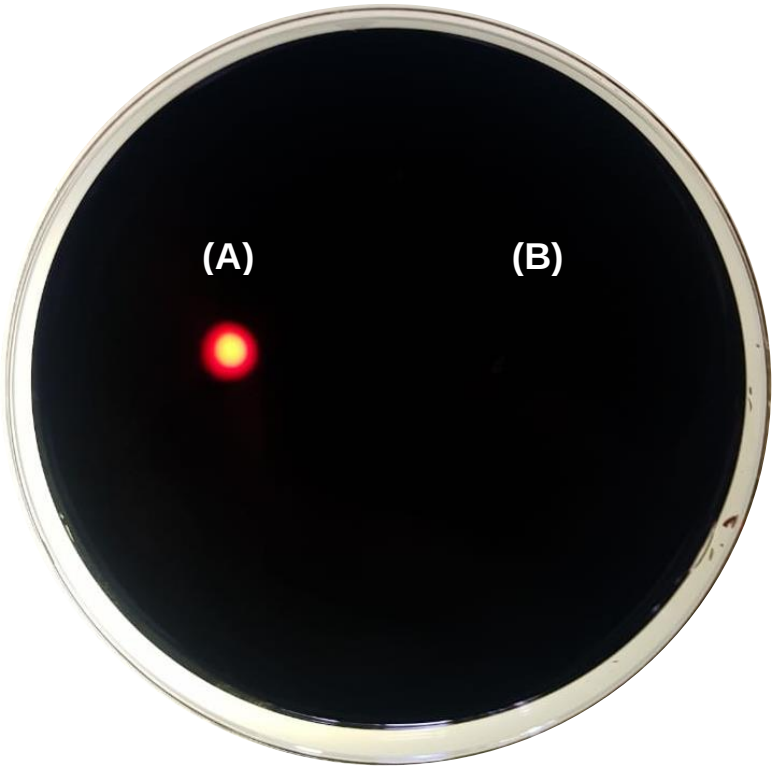

525

526

527 **Fig. 2**

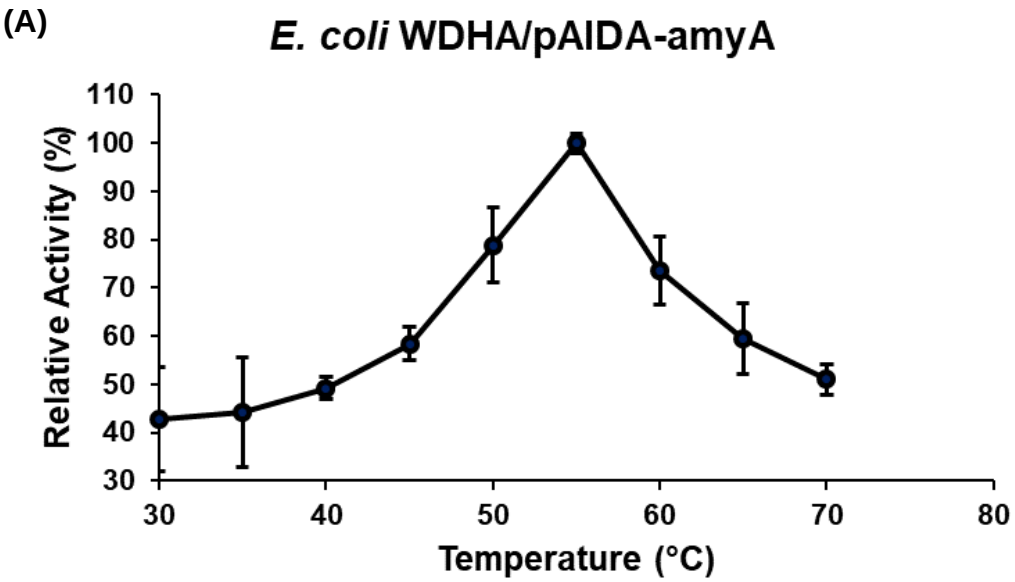

528

529

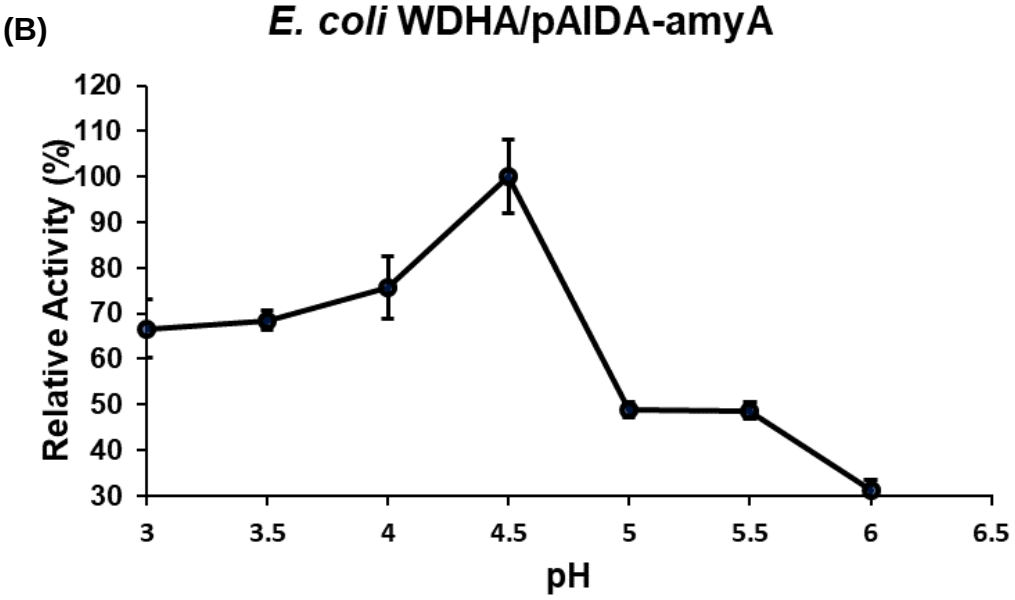

530

531 **Fig. 3**

532

533

534

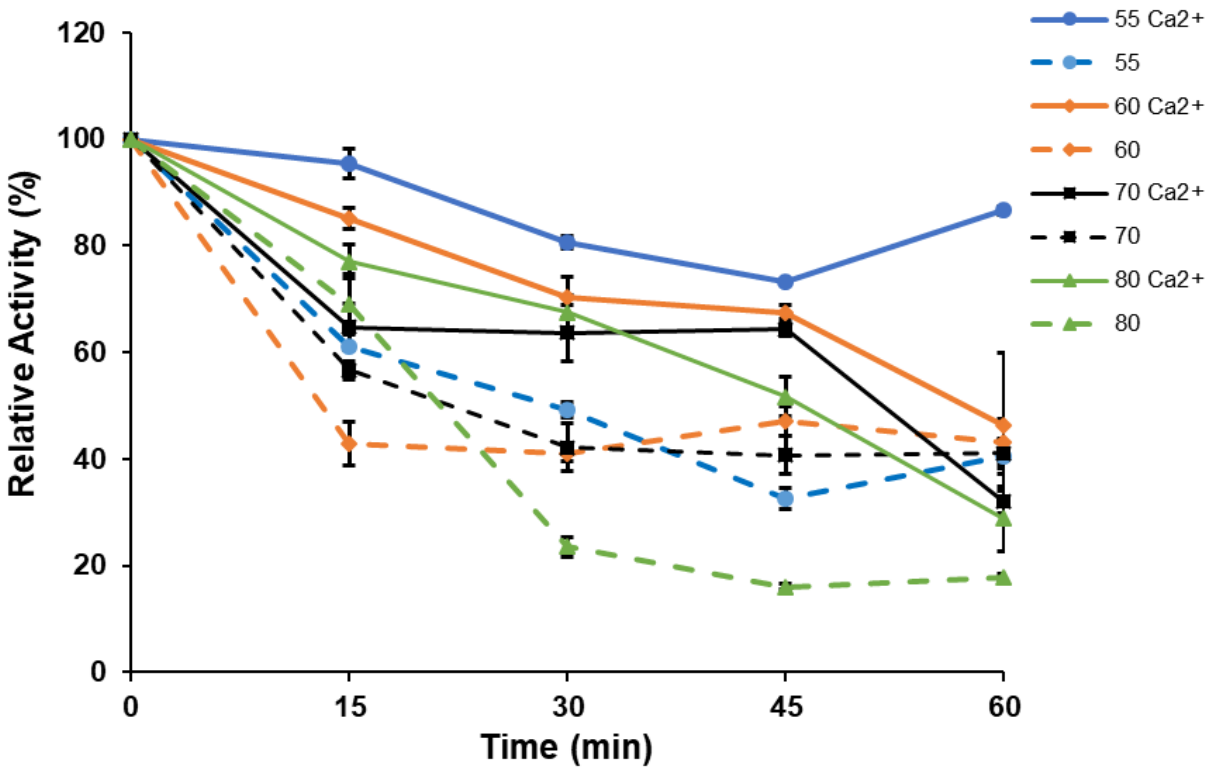

535

536

537 **Fig. 4**

538

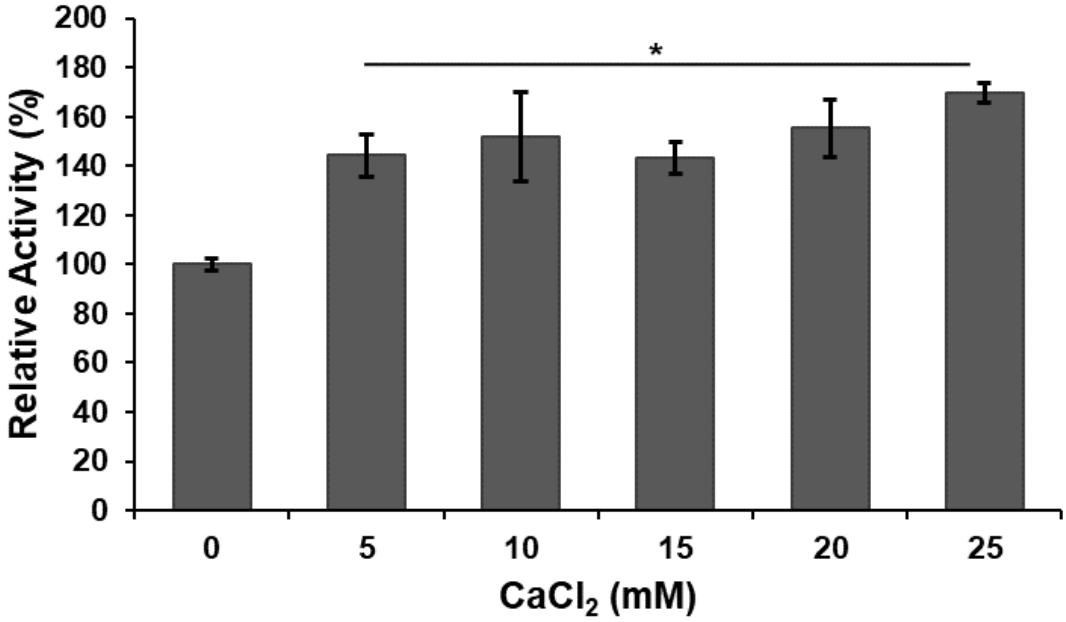

539

540 **Fig. 5**

541

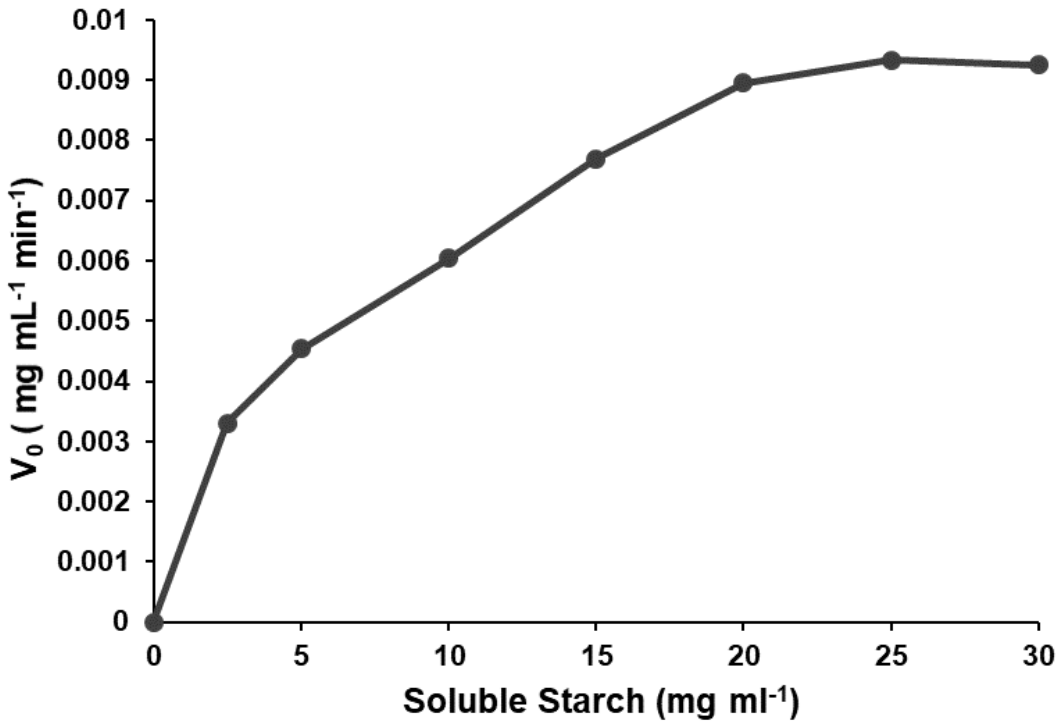

542

543 **Fig. 6**

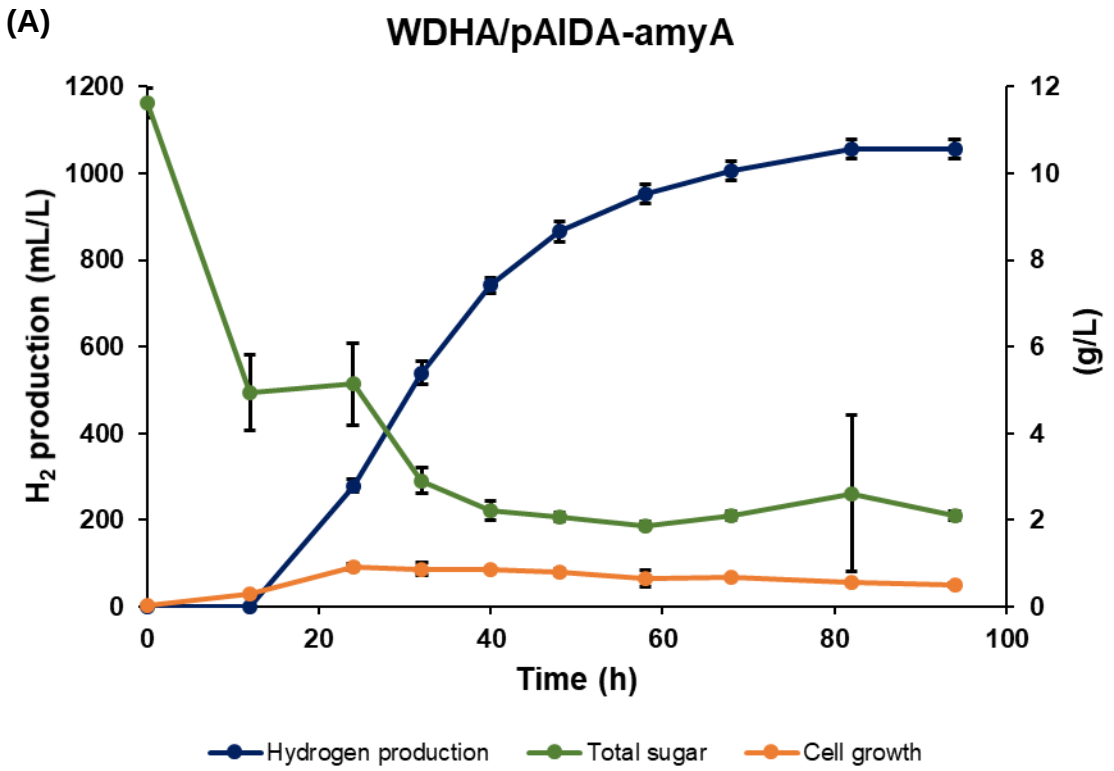

544

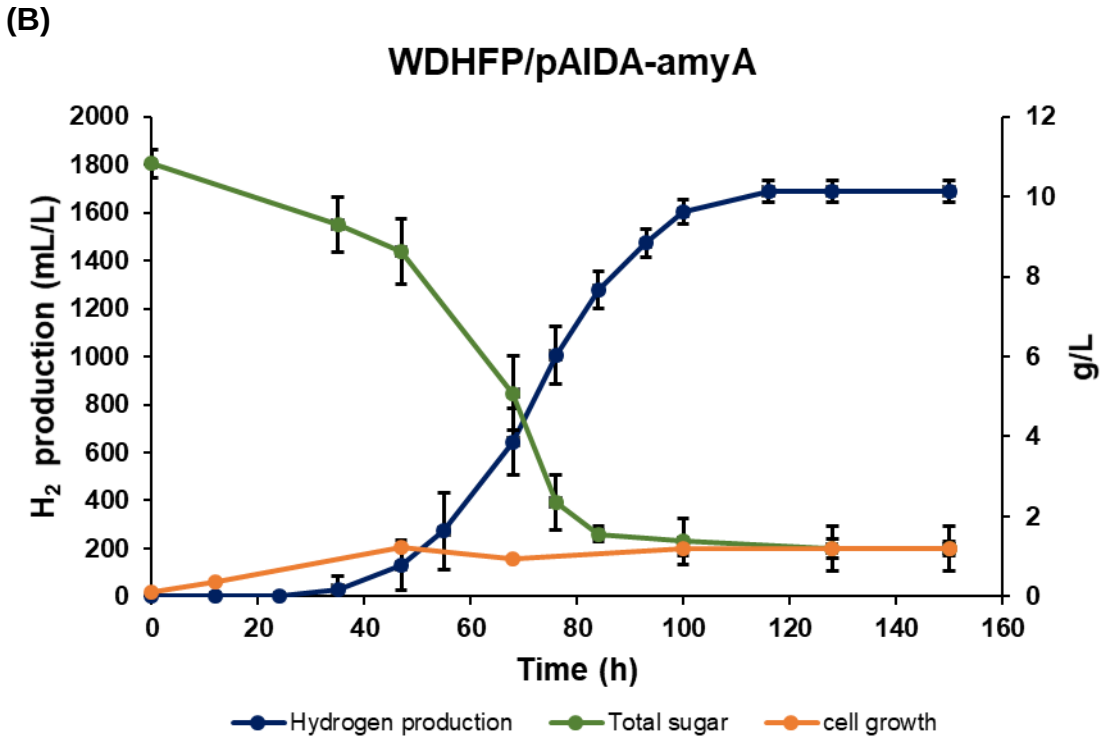

545

546 **Fig.7**

547

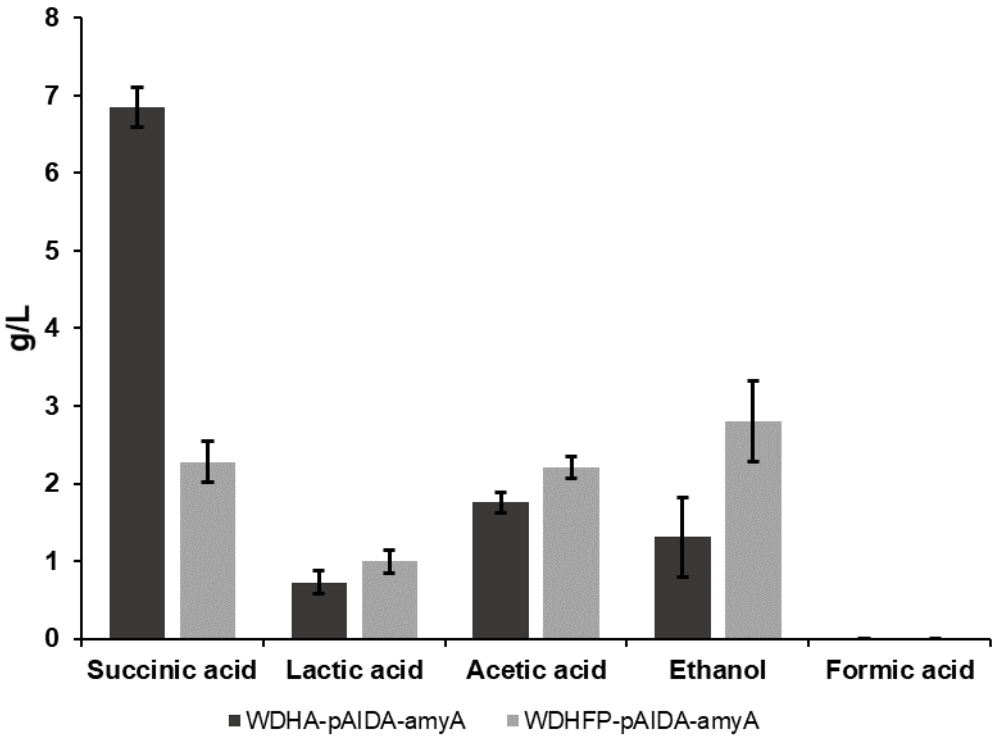

548

549 **Fig.8**